



**Fermi National Accelerator Laboratory**

**FERMILAB-Conf-96/350-E**

**CDF**

## **QCD Physics at CDF**

**Thomas Devlin**

**For the CDF Collaboration**

*Department of Physics and Astronomy,  
Rutgers — The State University of New Jersey  
Piscataway, New Jersey 08855-0849*

*Fermi National Accelerator Laboratory  
P.O. Box 500, Batavia, Illinois 60510*

October 1996

Published Proceedings of the *XXVIII International Conference on High Energy Physics*, Warsaw, Poland,  
July 25-31, 1996.



## **Disclaimer**

*This report was prepared as an account of work sponsored by an agency of the United States Government. Neither the United States Government nor any agency thereof, nor any of their employees, makes any warranty, express or implied, or assumes any legal liability or responsibility for the accuracy, completeness or usefulness of any information, apparatus, product or process disclosed, or represents that its use would not infringe privately owned rights. Reference herein to any specific commercial product, process or service by trade name, trademark, manufacturer or otherwise, does not necessarily constitute or imply its endorsement, recommendation or favoring by the United States Government or any agency thereof. The views and opinions of authors expressed herein do not necessarily state or reflect those of the United States Government or any agency thereof.*

## **Distribution**

*Approved for public release: further dissemination unlimited.*

THOMAS DEVLIN

*Department of Physics and Astronomy  
Rutgers - The State University of New Jersey  
Piscataway, NJ, 08855-0849 USA*

## REPRESENTING THE CDF COLLABORATION

The CDF collaboration is engaged in a broad program of QCD measurements at the Fermilab Tevatron Collider. I will discuss inclusive jet production at center-of-mass energies of 1800 GeV and 630 GeV, properties of events with very high total transverse energy and dijet angular distributions.

## 1 Introduction

The Tevatron Collider has produced collisions of antiprotons and protons at a center of mass energy of 1800 GeV. The Collider Detector at Fermilab (CDF) is a general purpose magnetic detector, used to study many aspects of these collisions. This talk presents high-statistics measurements of jet production over a wide range of transverse energy with low systematic uncertainties.

In 1992/93 we recorded  $19 \text{ pb}^{-1}$ , denoted "Run 1a." Results of Run 1a, containing details of the apparatus and analysis, were published.[1] (See Fig. 1)

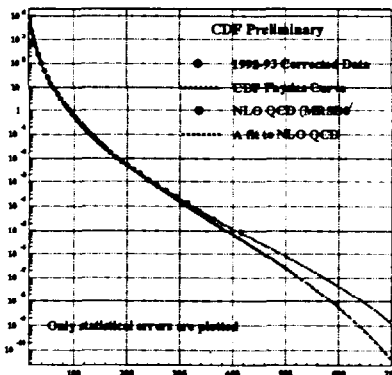


Figure 1: Inclusive jet cross sections from Run 1a

Results were in excellent agreement with theory up to jet transverse energies,  $E_T$ , of 200 GeV, but departed from theory at higher  $E_T$  where the gluon structure function is not constrained by independent data. In 1994/95 we recorded  $87 \text{ pb}^{-1}$ , denoted "Run 1b." A small sample of data taken in 1996, "Run 1c", included  $0.6 \text{ pb}^{-1}$  at a collision energy of 630 GeV. These newer results are discussed here.

These studies can be compared with calculations of quark and gluon interactions based on Quantum Chromodynamics (QCD) as the underlying theory of parton interactions. Presently, perturbative calculations of or-

der  $\alpha^3$  are available.[2] The measurements are sensitive to hadron structure as represented by parton distribution functions (PDF). This allows tests of consistency with other experiments such as deep inelastic scattering, hadronic final states in  $e^+e^-$  collisions and productions of  $\gamma$ 's,  $W$ 's and  $Z$ 's. Embedded in such calculations are assumptions about the validity of perturbation expansions, the running of the strong coupling constant ( $\alpha_s$ ), renormalisation and factorization, and soft-gluon resummations. At extremely high  $E_T$  one expects to be sensitive to short-range interactions, if they exist, at the level of  $10^{-17} \text{ cm}$ .

## 2 Inclusive Jet Production: 1800 GeV

We define the inclusive jet cross section as:

$$\frac{1}{\Delta\eta} \int d\eta \frac{d^2\sigma}{dE_T d\eta} = \frac{1}{\Delta\eta} \frac{1}{L} \frac{N_{jet}}{\Delta E_T}$$

where  $N_{jet}$  is the number of jets observed in a transverse-energy bin of width,  $\Delta E_T$ , with a weighted mean,  $E_T$ .  $L$  is the integrated luminosity. The range of pseudo-

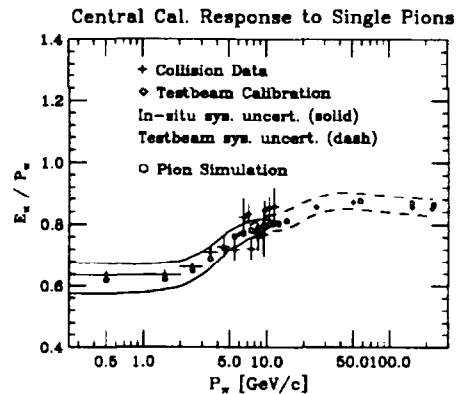


Figure 2: Corrections to energy scale.

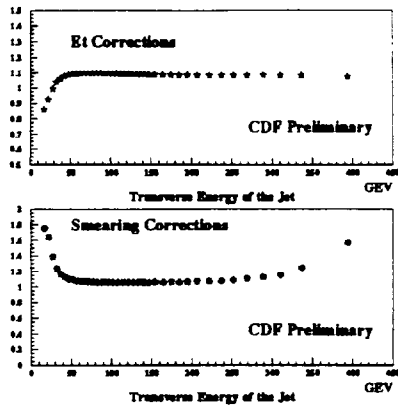


Figure 3: Corrections to cross sections from energy scale and energy smearing.

rapidity,  $\Delta\eta$ , uses a region of CDF's central calorimeter which minimizes edge effects,  $0.1 < |\eta| < 0.7$ .

The online trigger for events in this analysis required a single calorimeter cluster with  $E_T > 100$  GeV. Additional  $E_T$  thresholds of 70 GeV, 50 GeV and 20 GeV also contributed events with appropriate pre-scale factors to limit rates. Standard cleanup cuts were made to eliminate backgrounds, e.g. events with out-of-time calorimeter signals and events with significant missing  $E_T$ . Events were required to have an interaction vertex with  $|z| \leq 60$  cm from the detector center along the Tevatron beam axis.

For events which passed cuts, a histogram was formed as a function of jet  $E_T$ , and each jet in each event contributed to the histogram if it had  $E_T > 100$  GeV and  $0.1 < |\eta| < 0.7$ . All events with a jet above 200 GeV were scanned and no background events were found. We estimate that the background is less than 0.5% in any bin over the entire  $E_T$  spectrum. Small

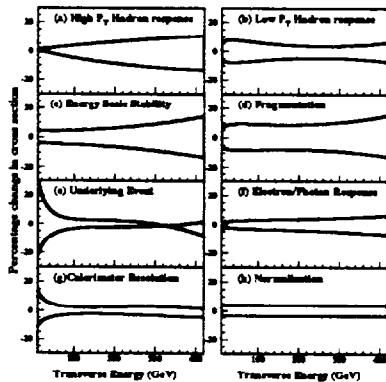


Figure 4: Correlated systematic uncertainties: percent vs.  $E_T$

inefficiencies near thresholds for each trigger were measured and values of the cross section and its uncertainty corrected. An overall normalization uncertainty of

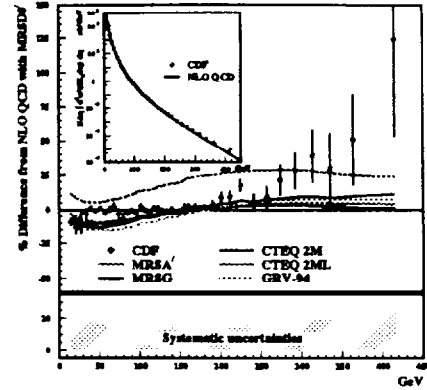


Figure 5: Linearized difference between measured cross section and theoretical predictions

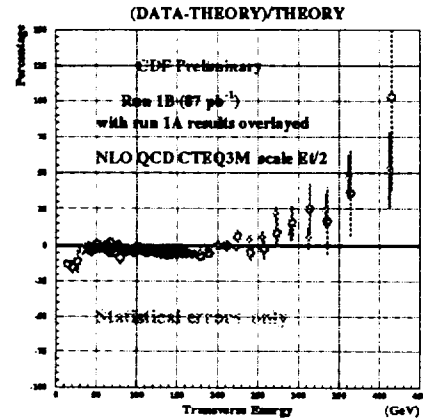


Figure 6: Cross sections from Run 1a and Run 1b compared with NLO QCD using CTEQ3M PDF's.

3.9% arises from the integrated luminosity and  $z$ -vertex cut. Extensive studies and cross checks were done to determine the proper jet energy scale for calorimeter information, and to correct the cross section for energy "smearing" events from finite resolution. Figures 2 and 3 show these effects. Overall, there were eight sources of systematic uncertainty, statistically independent of each other, but each fully correlated across all  $E_T$  bins. They are shown in Fig. 4. Any differences between experiments or between data and theory must include these effects for proper evaluation of significance.

The fully corrected cross sections for Run 1a are shown in Figures 1 and 5 and compared with NLO-QCD predictions using the MRSD0' Figure 6 shows results from Run 1b in good agreement with those from Run 1a. A comparison between CDF and D0 data, corrected for different  $\eta$  ranges is shown in Fig. 7 using JETRAD as the theoretical model. The CDF/D0 comparison is also done in Fig. 8 using CDF standard curve as the model for comparison. When systematic effects are included, there is no significant difference between the two experiments. Also shown are the CDF standard fitting function (used in  $E_T$  unsmearing) with best-fit parameters for the data

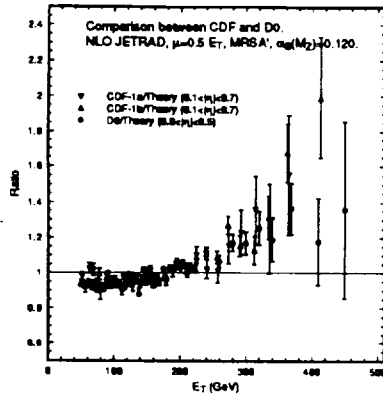


Figure 7: CDF and D0 Cross sections compared with JETRAD.

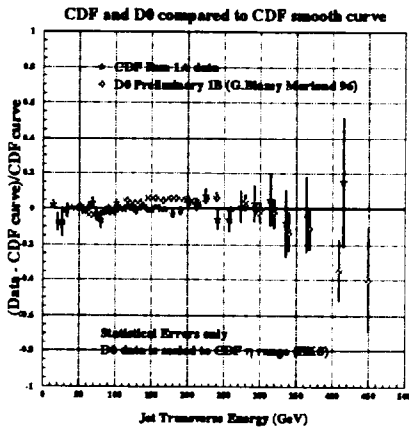


Figure 8: CDF and D0 Cross sections compared with CDF standard curve.

and for the MRSD0' curve.

The statistical significance of the difference between data and theory has been studied for various PDF's, including effects of systematic uncertainties.[1] MRSD0' gives the best agreement (C.L.=80%) For  $E_T$  between 40 and 160 GeV, but the C.L. is about 1% for data above 160 GeV. Other PDF's give up to 8% C.L. for the high  $E_T$  range, but poorer agreement at low  $E_T$ .

This apparent disagreement has stimulated theoretical work:

- New PDF's from CTEQ,[3]
- New calculation of effects of soft gluon resummation,[4]
- Evaluation of uncertainty in factorisation scheme,[5]
- Calculation of the running of  $\alpha_s$ .[6]

Other issues which might play a role in explaining the difference are the choice of  $\mu$ , the renormalisation/factorisation scale, new particles or a new short-range interaction.

### 3 High $\sum E_T$ Distributions

We have also measured the cross section as a function of  $\sum E_T$ , the scalar sum of jet  $E_T$  in an event for jets with  $E_T > 100$  GeV. Figures 9 and 10 show the results which also lie significantly higher than theoretical predictions for high  $\sum E_T$ .

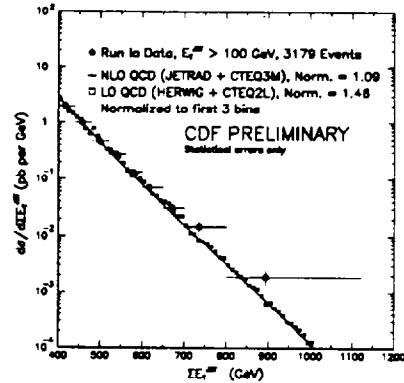


Figure 9: Cross section vs. the scalar sum of  $E_T$  for jets.

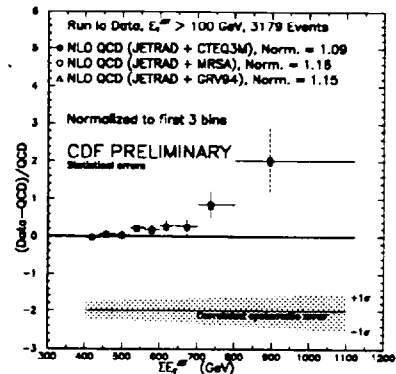


Figure 10: Cross section vs. the scalar sum of  $E_T$  for jets.

### 4 Candidates to Explain Excess at High $E_T$

In Fig. 11 we show a number of possible choices for  $\mu$ , the renormalisation/factorisation scale, based on jet  $E_T$ . The principal effect is almost shape independent. The D0 collaboration has used  $\mu$  based on the maximum jet  $E_T$  in the event which yielded a shape change with about a 5% to 10% higher cross section at 400 GeV.

The role of the running of  $\alpha_s$  has been studied,[6] and a fit to the jet cross sections up to  $E_T = 200$  GeV is shown in Fig. 12.

We have studied the effect of a short-range (contact) interaction characterised by the mass scale,  $\Lambda_c$ . At present such a calculation is available only in leading order. Figure 13 provides some idea of the value of  $\Lambda_c$  needed to explain what we observe.

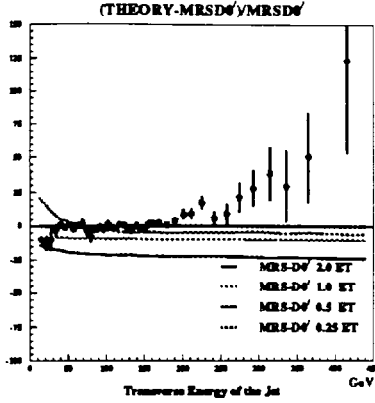


Figure 11: Theoretical predictions for various  $\mu$ -scales.

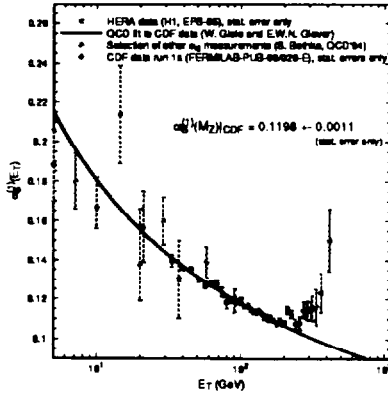


Figure 12: Calculations of  $\alpha_s$  from various experiments.

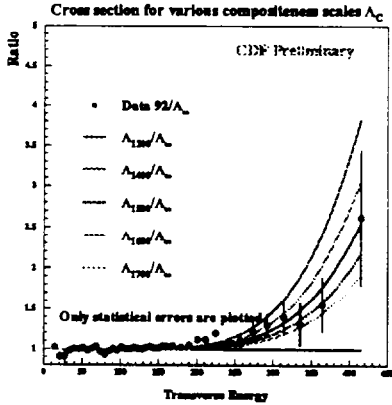


Figure 13: Effect of a contact interaction on theoretical prediction.

## 5 Dijet Angular Distributions

With several possible sources to explain the observed data-theory difference in the inclusive cross sections, it is not possible to sort out the proper combination of effects without other measurements to provide additional constraints. We have also measured the dijet angular distributions for the Run 1a and Run 1b data.[7] This is sensitive to the presence of a short-range contact interaction because the dominant QCD angular distribution

behaves as  $1/(1 - \cos \theta^*)^2$ , whereas a left-handed contact interaction has a contribution  $(1 + \cos \theta^*)^2 (\pi s)/(8\Lambda_c^4)$ . Other forms for a contact interaction may be possible, but this is the one we have studied.

It is customary to express the angular distribution in terms of

$$\begin{aligned} \chi &= \exp(|\eta_1 - \eta_2|) \\ &= (1 + |\cos \theta^*|)/(1 - |\cos \theta^*|) \end{aligned}$$

Figure 14 shows the  $\chi$  distributions for di-jets for various ranges of di-jet masses. Also shown are the NLO QCD predictions.

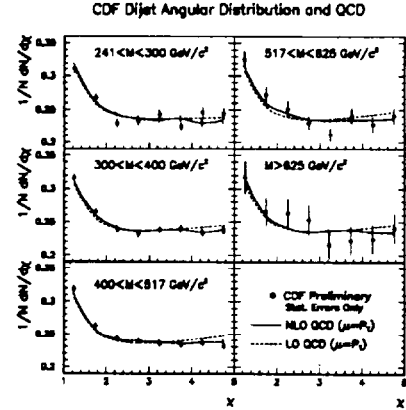


Figure 14: Dijet distributions in  $\chi$  for various dijet masses.

It is useful to integrate the differential  $\chi$ -distribution over the ranges  $1.0 < \chi < 2.5$  and  $2.5 < \chi < 5.0$ , and to form the ratio,  $R_\chi$ , of the lower range to the higher range.  $R_\chi$  is plotted in Fig. 15 along with predictions of

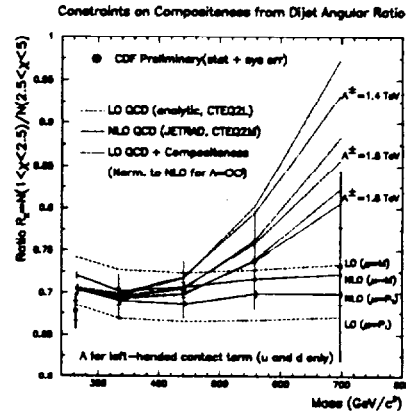


Figure 15: Ratio of  $\chi$  regions vs. dijet mass compared to predictions with contact interaction (u,d only) for various  $\Lambda_c$ .

a model with a contact interaction involving only u- and d-quarks and for various values of  $\Lambda_{uc}$ . At the 95% C.L., this model is excluded for  $\Lambda_{ud}(+) \geq 1.6$  TeV and for  $\Lambda_{ud}(-) \geq 1.4$  TeV, where (+) and (-) represent the two possible signs of the contact interaction. Figure 16 does the same thing for a flavor-symmetric model where the

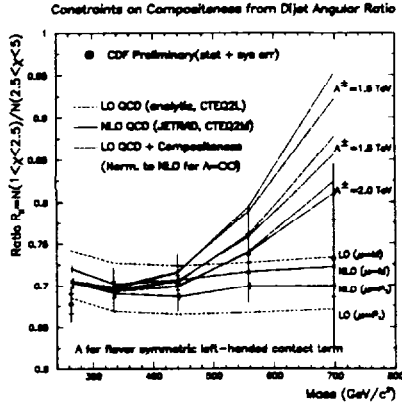


Figure 16: Ratio of  $\chi$  regions vs. dijet mass compared to predictions with contact interaction (flavor symmetric) for various  $\Lambda_c$ .

corresponding limits are:  $\Lambda(+)$   $\geq$  1.8 TeV and  $\Lambda(-)$   $\geq$  1.6 TeV.

These results argue against a new short-range interaction of this type as the dominant source of the effect seen in the inclusive jet cross section.

## 6 High $\sum E_T$ Multijet Distributions

We have also studied detailed kinematic distributions of the multijet events discussed earlier. The data are compared with two QCD models: NJETS, a LO  $2 \rightarrow N$  Monte Carlo calculation,[8] and with the HERWIG MC[9]. As alternate to QCD, we also plot the predictions for phase space. For  $N=3$ , the process  $1+2 \rightarrow 3+4+5$  is characterized by variables described in Ref. [10]. For jets 3, 4 and 5 ordered in energy, they are the 3-jet invariant mass, two Dalitz variables, the angle between  $\vec{P}_1$  and  $\vec{P}_3$  the angle between plane  $S_{123}$  containing  $\vec{P}_1, \vec{P}_2$  and  $\vec{P}_3$  and plane  $S_{345}$  containing  $\vec{P}_3, \vec{P}_4$  and  $\vec{P}_5$ , and the three mass fractions:  $f_j = M_j/M_{3J}$ ,  $j = 3, 4, 5$ . The 4-Jet ('') and 5-Jet ('') events are reduced to the equivalent 3-Jet case by combining successively, the lowest-mass jet pairs.

In Figs. 17 18 and 19 we show a sample of a much larger list of distributions.[11] These distributions are

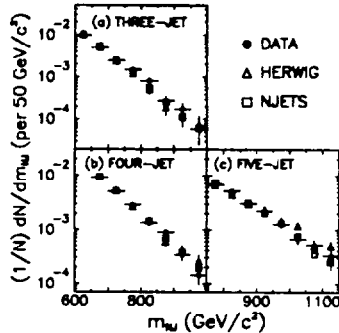


Figure 17: N-jet mass distributions for 3-, 4- and 5-jet events.

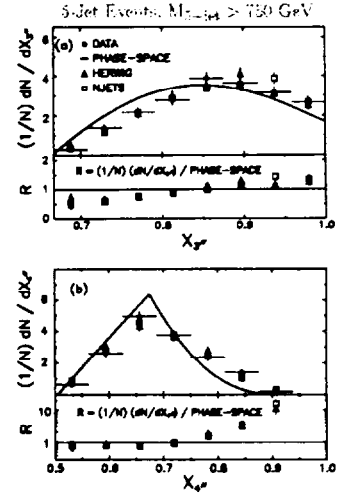


Figure 18: Dalitz-variable distributions for 5-jet events.

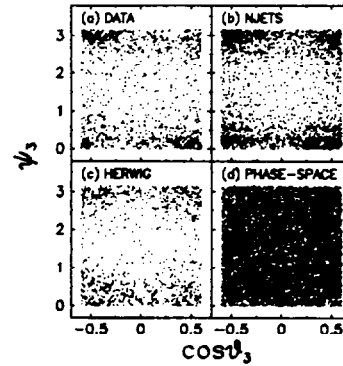


Figure 19: Angular distributions for 3-jet events.

consistent with the QCD predictions, and they give no hint of new physics.

## 7 Recent CTEQ PDF Fits

A number of theoretical groups are calculating new PDF's as more precise data emerge from deep inelastic scattering (DIS), HERA, W-asymmetry measurements, Drell-Yan studies, direct photon interactions and high energy jet production. The kinematic range covered by various experiments is shown in Fig. 20.[3]

Other talks at this conference will describe this work, but I cannot resist the temptation to show data-theory comparisons with the inclusive jet cross section based on two recent fits by CTEQ in Fig. 21. The jet data from CDF and D0 are included in the CTEQ4M solution which still shows a suggestion of a rise in the cross section at high  $E_T$ . The CTEQ4M fit to data from many experiments has  $\chi^2/d.f = 1320/1297$ . Although somewhat constrained by theory, the exact functional form for the PDF's is a matter of convenience and judgement. Data at low  $x$  can strongly constrain the parameters of the fit and

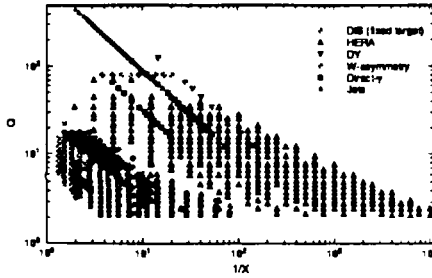


Figure 20: Kinematic regions covered by various experiments used in CTEQ fits.

overwhelm the influence of the high- $E_T$  jet data which are the only constraints on the high- $x$  part of the gluon PDF. In the CTEQHJ fit, the statistical weights of the jet data were arbitrarily increased to force good agreement at high  $E_T$  as seen in the figure. This resulted in  $\chi^2/d.f. = 1343/1297$ , still in rather good agreement with data from other experiments.

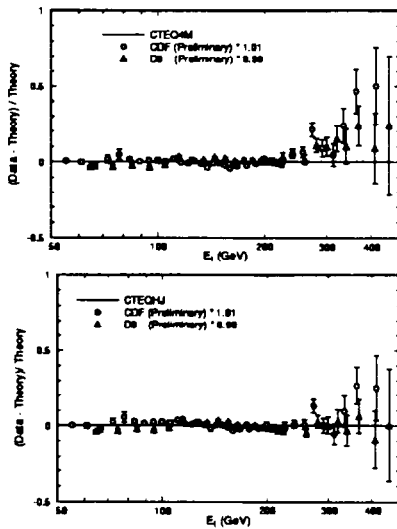


Figure 21: CTEQ fits including inclusive jet data.

### 8 Inclusive Jet Production: 630 GeV

In a 1989 CDF run, we collected data at a c.m. energy of 546 GeV as a test of scaling in the variable,  $x_T = 2E_T/\sqrt{s}$ . [12] QCD predicts scaling violation and the experiment was consistent with that at high  $x_T$ , but there was a hint that the violation at low  $x_T$  was not as strong as expected from QCD. Run 1c produced a sample of jet events at 630 GeV which is shown in Figs. 22. A comparison with NLO QCD using the MRSA' PDF is given in Fig. 23 vs.  $x_T$ , and a the newer CTEQ3M PDF is shown in Fig. 24 where the results are plotted vs.  $E_T$ .

A direct comparison 1800 GeV data and 630 GeV data which removes some sources of systematic error is shown in Fig. 25 compared with the CTEQ3M prediction

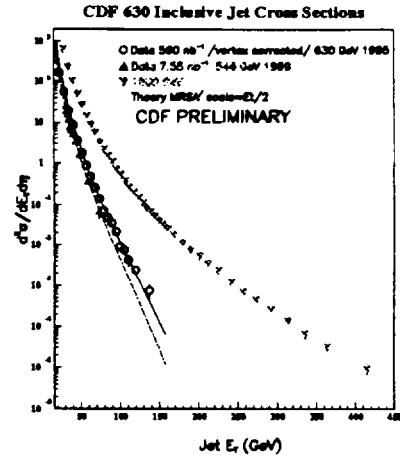


Figure 22: Inclusive jet cross sections at various c.m. energies.

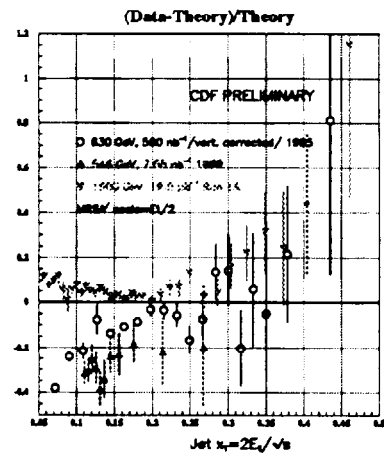


Figure 23: Inclusive jet cross sections: difference from theory at various  $x_T$ .

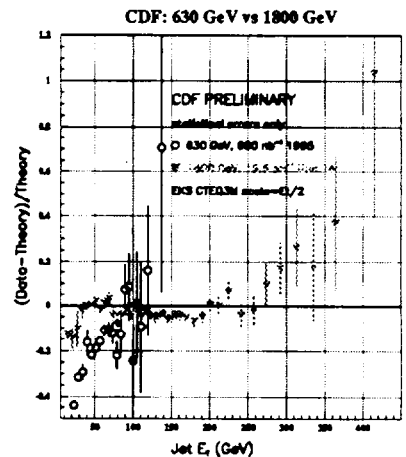


Figure 24: Inclusive jet cross sections: difference from theory at various  $E_T$ .

for this ratio. Comparisons with UA2 data taken at 630 GeV are difficult because of different jet algorithms and



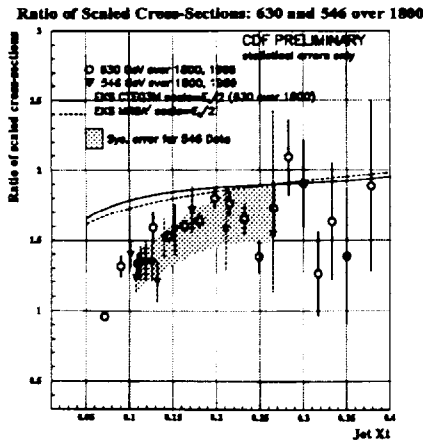


Figure 25: Experimental ratio of CDF jet cross section at 630 GeV to that at 1800 GeV.

different jet energy corrections in use at that time.

These results suggest that more work is needed to understand scaling behavior at low jet  $x_T$ .

## 9 Conclusions

These new measurements of jet production at high  $E_T$  are an exciting challenge which is leading to refinements in QCD theory. The inclusive jet cross sections probe a region of gluon structure functions not constrained by other data. While new PDF fits can account for the high  $E_T$  behavior, we cannot be sure that this is the correct explanation for the high  $E_T$  behavior. Detailed distributions of di-jets and multi-jets with respect to a variety of kinematic parameters are in good agreement with theory. The  $x_T$  scaling behavior for 630-GeV and 1800-GeV data deviate from QCD predictions at low  $E_T$ . We look forward to improvements in both theory and experimental data.

## Acknowledgments

I am grateful for the efforts of my colleagues in Rutgers, CDF and Fermilab. This work was supported in part by the United States Department of Energy, and by the National Science Foundation. (Note: The complete set of figures, including some omitted here can be found in <http://www.physics.rutgers.edu/devlin> along with a related talk the following month.)

## References

1. F. Abe et al., Phys. Rev. Lett. **77**, 438 (1996).
2. S. Ellis et al., Phys. Rev. Lett. **64** 2121(1990); F. Aversa et al., Phys. Rev. Lett. **65**, 401 (1990); W. T. Giele et al., Nucl. Phys. **B403** 633 (1993).
3. H.L. Lai et al. e-print hep-ph/9606399
4. S. Catani et al., eprint hep-ph/9604351
5. M. Klasen and G. Kramer e-print hep-ph/9605210
6. W. Giele et al., Phys. Rev. **D53**, 110 (1996)
7. F. Abe et al., (The CDF Collaboration) Fermilab-PUB-96/317-E.
8. F.A. Behrends and H. Kuijff, Nucl. Phys. **B353**, 59 (1991).
9. G. Marchesini and B. Webber, Nucl. Phys. **B310**, 461 (1988).
10. S. Geer and T. Asakawa, Phys. Rev. **D53**, 4793 (1996).
11. F. Abe et al. Phys. Rev. Letters **75**, 608 (1995); F. Abe et al., submitted to Phys. Rev. D, FERMILAB-PUB-96/098-E.
12. F. Abe et al., Phys. Rev. Lett. **70**, 1376 (1993).